Estimation of methane emission from West Siberian wetland by scaling technique between NOAA AVHRR and SPOT HRV

Wataru Takeuchi[a,*], Masayuki Tamura[b], Yoshifumi Yasuoka[a]

[a] Institute of Industrial Science, University of Tokyo, Japan
[b] National Institute for Environmental Studies, Japan

Abstract

Wetlands are one of the most important ecosystems in the world and at the same time they are presumed to be a source of methane gas, which is one of the most important greenhouse gases. The West Siberian wetlands is the largest in the world and remote sensing techniques can play an important role for monitoring the wetland.

High spatial resolution satellite data are effective for monitoring land cover type changes, but can't cover a wide area because of a narrow swath width. On the other hand, global scale data are indispensable in covering a large area, but are too coarse to get the detailed information due to the low spatial resolution. It is necessary to devise a method for the fusion of the data with different spatial resolutions for monitoring the scale-differed phenomena.

In this paper, firstly, a SPOT HRV image near Plotnikovo mire was used to map four wetland ecosystems (birch forest, conifer forest, forested bog and open bog) supplemented by field observation. Then, spectral mixture analysis was performed between NOAA AVHRR and SPOT HRV data acquired on the same day.

Secondly, field observations were scaled up with these different spatial resolution satellite data. Each of the wetland ecosystem coverage fraction at the sub-pixel level was provided by spectral mixture analysis. Field observation shows that the mean rate of CH_4 emission from forested bog and open bog averaged 21.1 and 233.1 (mg CH_4/m^2/day), respectively. The methane emission from the area was estimated by multiplying these average methane emission rates and the fraction coverage in each AVHRR pixel.

Finally, the total methane emission over AVHRR coverage was estimated to be 9.46 (10^9 g CH_4/day) and the mean methane emission over AVHRR coverage was calculated as 59.3 (mg CH_4/m^2/day). We could conclude that this mean value is within the probabilistic variability as compared with the airborne measurement results.
© 2003 Published by Elsevier Science Inc.

Keywords: West Siberia; Wetland; Spectral mixture analysis; Scaling up; Methane emission

1. Introduction

Methane is a particularly effective greenhouse gas whose atmospheric concentration is increasing at a rate of approximately 1% per year, yet its source strengths are still poorly quantified. The most comprehensive assessment of global sources of atmospheric methane and their future dynamics has been conducted by United Nation's Intergovernmental Panel on Climate Change (IPCC). The IPCC data suggests that natural wetlands are now responsible for approximately 21% of global methane emissions (Houghton et al., 1998). In situ measurements suggest that northern high-latitude wetlands may be a major source of methane gas due to anaerobic bacterial decomposition in water-logged peat lands. Since its global warming potential is very high, estimation of methane from different sources is now one of the urgent tasks in addressing the problem of global warming. Wetlands are presumed to be a major emission source of methane and estimation of methane emission requires precise assessment of wetlands in global or continental scale (Singh, Kulshrestha, & Agnihotri, 1991). It is, however, not easy to investigate

wetland distribution with only ground observations because it is usually extensive and difficult to traverse. Remote sensing of wetland from satellites may play an important role in monitoring wetland conditions and to distinguish wetland from other land cover types.

There have been several studies to produce land cover maps of individual wetlands by using remote sensing data with high spatial resolutions such as Landsat MSS or TM, SPOT HRV or JERS-1 SAR. High spatial resolution data are effective in monitoring wetland environment at the local or regional scale, however, it may not cover a large area because of its narrow swath width. Another obstacle to mapping the world with high-resolution data is the cost and logistics of handling the data volume. Extending the area would require use of wide coverage data such as NOAA AVHRR or TERRA MODIS. On the other hand, AVHRR data may not detect fine spatial structures in mixtures of vegetation, soil and water in wetland because of its coarse spatial resolution. In this sense, it is necessary to devise a method for the fusion of the data with different spatial resolutions.

In this research, a scaling technique is investigated to unmix each pixel in low spatial resolution data into different land cover types including wetlands and forests, and to estimate the area cover ratio of wetland in each pixel. A scaling model relates the data with different spatial resolutions and extrapolates the local information on land cover types derived from high spatial resolution data to global scale through low spatial resolution data. Here, we used two types of satellite sensors: SPOT HRV as a high spatial resolution sensor and NOAA AVHRR as a low spatial resolution sensor. High spatial resolution data (HRV) is used for classifying the land cover types in detail and formulating a scaling model between NOAA AVHRR and SPOT HRV. Global scale data (AVHRR) is used to monitor

the whole West Siberian wetland. Total methane emission from AVHRR area was calculated from the methane flux in situ measurements of two different types of bogs.

2. Study area and data description

2.1. Study area

West Siberian Lowland was selected as a test site since it is one of the largest wetlands in the world and is recognized as a high potential area for methane emission due to global warming. This area is mainly covered with forest and wetland. The wetland belongs to a belt of ombrotrophic sphagnum bogs of West Siberia. Bogs are peat-producing wetlands in moist climates, where organic material has accumulated over long periods. Their main feature is characterized by water and nutrient input into the system which is entirely through precipitation. They are extremely acid and nutrient-deficient (Crill et al., 1988). In this study, two types of bogs are subjectively defined which are subject to the estimation of methane emission. The difference between the two types of bogs is mainly characterized by water depth. Forested bog is mainly composed of shrub, where the water position is relatively lower. Open bog is mainly composed of lichens such as sedge or peat moss, where the water position is relatively higher. Birch trees are dominant in forested areas and coniferous forests are found along rivers.

During the summers of 1993, 1994 and 1995, several field studies were carried out near Plotnikovo, which is located in the southern part of West Siberian Lowlands (Fig. 1). The ground observation data have been compiled in collaboration with the Moscow Institute of Microbiology (Tamura & Yasuoka, 1998). They include methane emission
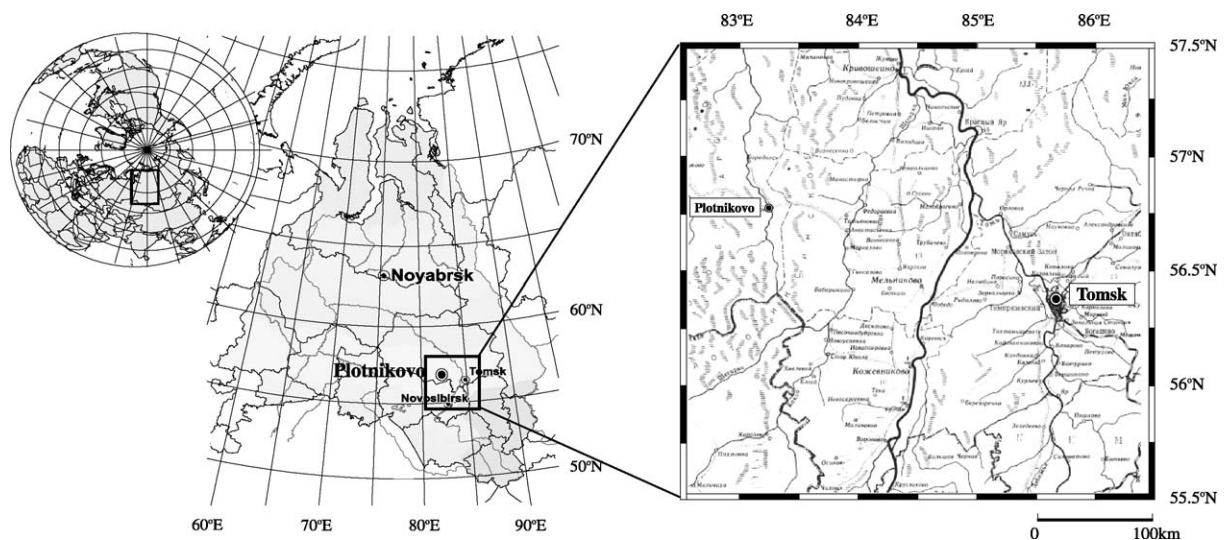
Fig. 1. Location of study area in the West Siberian Lowland.

from wetlands, soil temperature and a water acidity (pH). This ground survey and the aerial photographs provided the bulk of validating the data for image classification.

2.2. Methane flux measurement

To estimate the methane emission from the AVHRR area, we use the methane flux data measured on the ground. The two measurement sites for open bogs are indicated by circle symbols in Fig. 2. At the same time, vertical profiles of atmospheric methane concentration above SPOT coverage was conducted using an observation aircraft (Tohjima, Maksyutov, Machida, & Inoue, 1994). The white curve in Fig. 2 shows the flight pass of the airplane on August 5, 1994. The measurements for the other open bog and forested bogs were made outside the SPOT image area. Each microsite was positioned by a stainless steel square collar (area 40×40 cm^2, the depth of insertion into peat 10 cm). It was permanently installed before the start of the daily measurements. Net CH$_4$ flux was determined by the static chamber technique (Panikov, 1994). Air and soil temperature were measured by mercury thermometers and water acidity (pH) was determined with ion-selective electrodes.

2.3. Satellite data used in this study

SPOT HRV (green, red and near infrared channels) were used for wetland classification because it has a high resolution of 20 m. They were not calibrated to reflectance values. AVHRR channel 1 and 2 were calibrated to

Fig. 2. SPOT/HRV image at Plotnikovo (R/G/B = 2:3:1). Circle symbols show ground measurement points of methane fluxes. White curve shows flight pass of the airplane.

reflectance values and channel 3 to brightness temperature using coefficients based on NOAA KLM Users guide (Goodrum, Kidwell, & Winston, 1999) and cloud-free areas were selected carefully. Atmospheric and BRDF corrections were not performed. Pixels over 45° of the sensor scan angle were considered as unacceptable for processing. Both HRV and AVHRR data were acquired on July 7, 1995.

AVHRR data were geometrically corrected based on ground control point (GCP) matching by using PaNDA software, and registration error over the image was less than 1 pixel. PaNDA is a free software package for NOAA data analysis (Shimoda et al., 1998). HRV data were geometrically corrected and overlayed so that one pixel of AVHRR (1.1 km) covers a set of HRV pixels in a rectangular block of 55×55. RMS errors of image-to-image registration between HRV and AVHRR were 38 pixels in HRV size (20 m), which means 0.68 pixels in AVHRR size (1.1 km).

3. Land cover characterization method

3.1. Linear mixture model

The NOAA AVHRR is one of the few space-borne sensors currently capable of acquiring radiometric data over a broad range of view angles. However, the relatively coarse spatial resolution of the AVHRR ($1.1-4.3$ km) most often results in measurements of mixed land covers, and thus the pixel unmixing is indispensable (Asner, Wessman, & Priette, 1997; Bateson, Asner, & Wessman, 2000). Basically, a scaling model is focused on the unmixing of AVHRR pixel from high-resolution data, and each category area ratio in one AVHRR pixel is the most basic and important data (Price, 1999; Shimabukuro & Smith, 1991).

Let a remote sensing data have n channels and the coverage be composed of k types of categories ($\omega_1, \ldots, \omega_k$). Let the spectral characteristic of the category ω_i be expressed by the n dimensional spectral vector $\boldsymbol{m}_i$ ($i = 1, \ldots, k$). If the pixel $\boldsymbol{p}_{\mathrm{lm}}$ is composed of one category ω_i (pure pixel), then $\boldsymbol{p}_{\mathrm{lm}} = \boldsymbol{m}_i$. Linear spectral mixture analysis models the reflectance spectrum of each pixel in an AVHRR image in terms of endmember reflectance according to the equations and constraints below (Oleson et al., 1995)

$$\boldsymbol{p}_{\mathrm{lm}} = \sum_{i=1}^{k} a_{\mathrm{lm}}^{i} \boldsymbol{m}_i \qquad (1-\mathrm{a})$$

where

$$a_{\mathrm{lm}}^{i} \geq 0, \quad (i = 1, \ldots, k) \qquad (1-\mathrm{b})$$

$$\sum_{i=1}^{k} a_{\mathrm{lm}}^{i} = 1 \qquad (1-\mathrm{c})$$
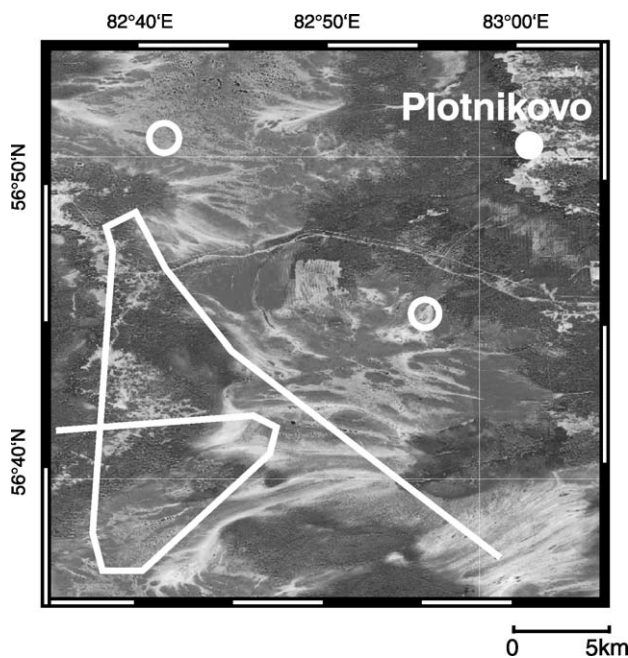
where a_{lm}^i is the fractional coverage of the category ω_i in the pixel. Eq. (1-a) is called the category combination, which is the combination of the spectral characteristics of multiple categories by the space average. In this case, the pixel data p_{lm} is expressed by the linear combination of the area ratio a_{lm}^i Eq. (1-b) expresses the positivity constraint of each category, and Eq. (1-c) the constraint equation of each category ratio, respectively. If the number k of endmembers equals the number of bands plus one, then in Eqs. (1-a) and (1-c) above, there are k equations in k unknowns, which can be uniquely inverted to solve for the a_{lm}^i in Eq. (1-a).

3.2. Quadratic programming problem

Because all of the fractions should sum to unity, a constraint equation can be incorporated into the problem as well as positivity constraints on the fraction estimates. Apart from indirect applications, there are several classes of problems that are naturally expressed as quadratic problems. Examples of such problems can be found in planning, scheduling, game theory and many problems in economics (Floudas & Visweswaran, 1995). The general quadratic programming method is to give an answer a_{lm} with the non-negative condition. Objective function $Q(a_{\mathrm{lm}})$ is defined as follows

$$Q(a_{\mathrm{lm}}) = \frac{1}{2}a_m^t \mathbf{D} a_{\mathrm{lm}} + \mathbf{C}^t a_{\mathrm{lm}} \qquad (2-a)$$

where

$$\mathbf{D} = [D_{ij}] = [2(\mathbf{m}_i, \mathbf{m}_j)] \qquad (2-b)$$

$$\mathbf{C}^t = -2[(\mathbf{p}_{\mathrm{lm}}, \mathbf{m}_1), \dots, (\mathbf{p}_{\mathrm{lm}}, \dots, \mathbf{m}_k)] \qquad (2-c)$$

with the condition

$$a_{\mathrm{lm}}^i \geq 0, \quad (i = 1, \dots, k) \qquad (3-a)$$

$$\sum_{i=1}^{k} a_{\mathrm{lm}}^i \leq 1 \qquad (3-b)$$

$$\sum_{i=1}^{k} a_{\mathrm{lm}}^i \geq 1 \qquad (3-c)$$

If the matrix $\mathbf{D}$ is positive definite, Eq. (2-a) becomes a convex programming problem. Since any local optimum is equivalent to the global optimum in convex problems, there are many algorithms for convex quadratic programming. In this study, a gradient ascent algorithm (Uzawa algorithm) was applied to the dual functional with augmented Lagrangian (Elman & Golub, 1994).

4. Results and discussion

4.1. Classification of HRV data

For ecosystem characterization, four categories were selected including birch forest, conifer forest, forested bog and open bog. As described in Section 2.1, two categories for bogs were selected with respect to methane emission characteristics. Firstly, around 30 training areas were selected for each class on the basis of the GPS locations. All of the field data points were used to train the classifier. Then, the entire image of HRV was classified into four categories including birch forest, conifer forest, forested bog and open bog by using supervised classification. Fig. 3 shows the classification result.

4.2. Spectral mixture analysis

The ordinary least squares method was applied to solve for a mean AVHRR reflectance representative of the entire scene using Eq. (1-a). The coefficients represent the derived reflectances (endmembers) in Eq. (4-a–4-c). Fig. 4 shows the scatter plot between channels 1, 2 and 3, and the polygons drawn on the data domain are endmembers.

$$AV_1 = 5.04\ V_1 + 5.20\ V_2 + 8.75\ B_1 + 11.3\ B_2$$
$$R = 0.81 \qquad (4-a)$$

$$AV_2 = 47.5\ V_1 + 33.7\ V_2 + 32.4\ B_1 + 41.1\ B_2$$
$$R = 0.93 \qquad (4-b)$$

$$AV_3 = 21.2\ V_1 + 23.0\ V_2 + 46.5\ B_1 + 36.8\ B_2$$
$$R = 0.79 \qquad (4-c)$$

where AV_1 and AV_2 are reflectance values of AVHRR channel 1 and 2, AV_3 is brightness temperature value of
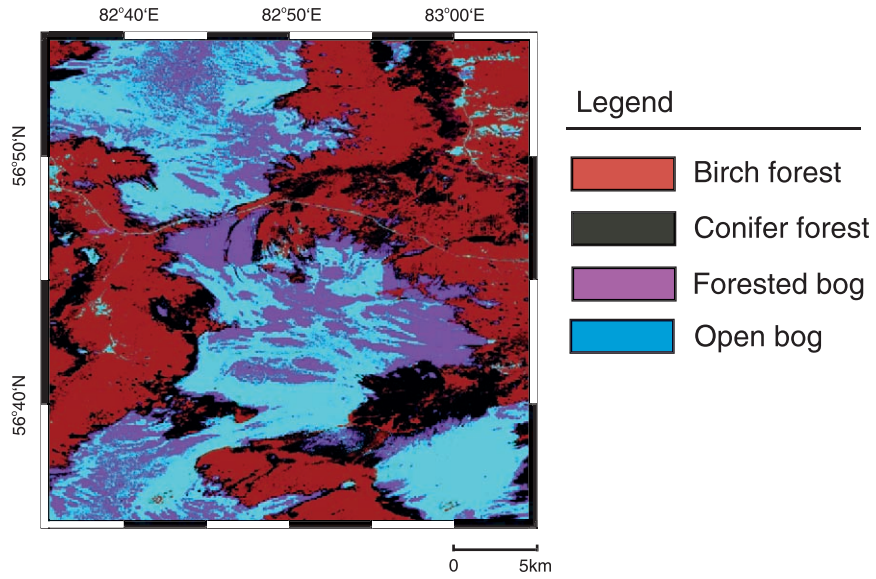
Fig. 3. Classification image of SPOT/HRV.
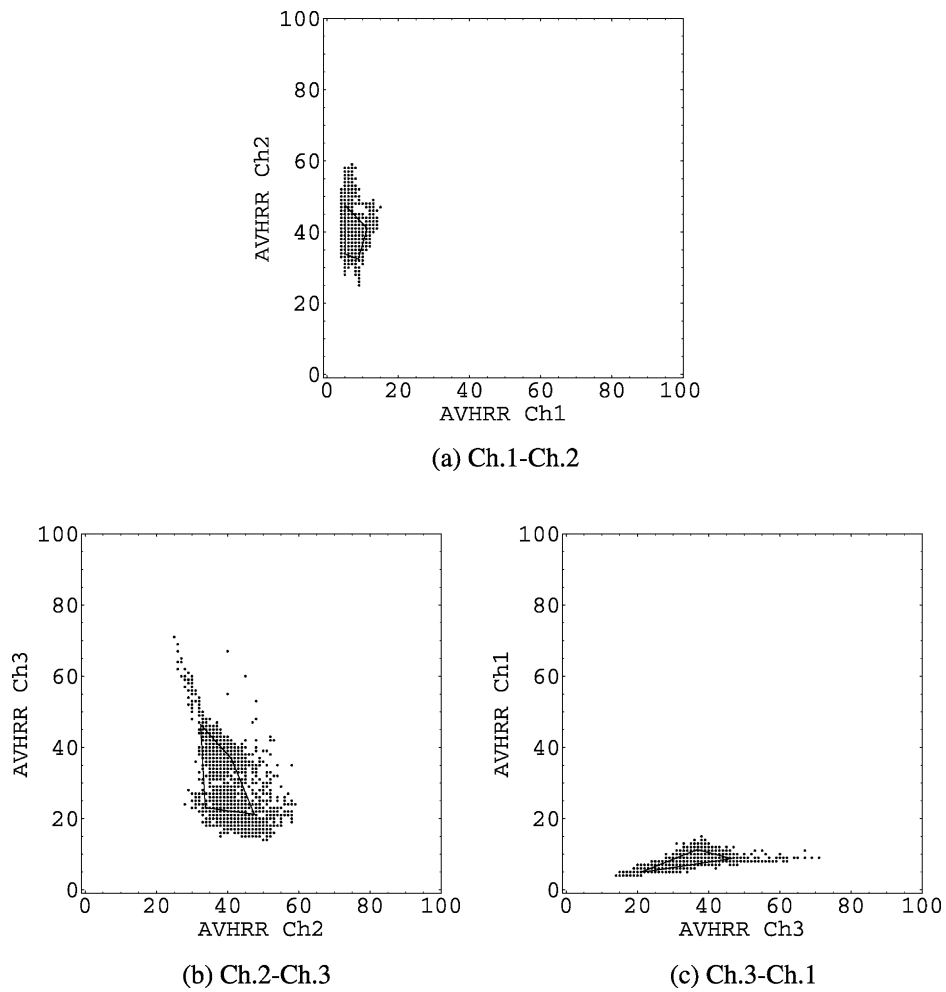
Fig. 4. Scatter plot of AVHRR channels 1, 2, and 3 reflectance values. The polygons drawn on the data domain are derived endmembers. Four corner points correspond to derived four endmembers in each scatter plot.

AVHRR channel 3. V_1, V_2, B_1 and B_2 are the fractional coverage of birch forest, conifer forest, forested bog and open bog respectively. R is the coefficient of correlation.

4.3. Estimation of forest and bog distribution

The derived scaling model was applied to generate maps showing the distribution of spectrally distinct chaparral birch forest, conifer forest, forested bog and open bog to the whole AVHRR data. By solving the derived Eq. (4-a–4-c) and Eq. (1-c), which shows the fractions sum to unity simultaneously, fractional coverages of each class were calculated. Fig. 5 presents the result of spectral mixture analysis. As a comparison, the original AVHRR image is shown in Fig. 6. From this

result, each category area was estimated as shown in Table 1.

4.4. Estimation of the methane emission

The results obtained in spectral mixture analysis enable us to scale up the ground measurements of methane emission to areas covered by AVHRR. Table 2 shows the mean methane emission rates observed in July of 1993 and 1994. The emission rate for forested bog and open bog were set 21.1 and 233.9 (mg CH_4/m^2/day), respectively. The emission rate for birch and conifer forests were set to zero because it is reported that forests do not release much methane, and in many cases, consume atmospheric methane at very low rates (Bartlett & Harris, 1993).

(a) Birch forest

(b) Conifer forest

(c) Forested bog

(d) Open bog
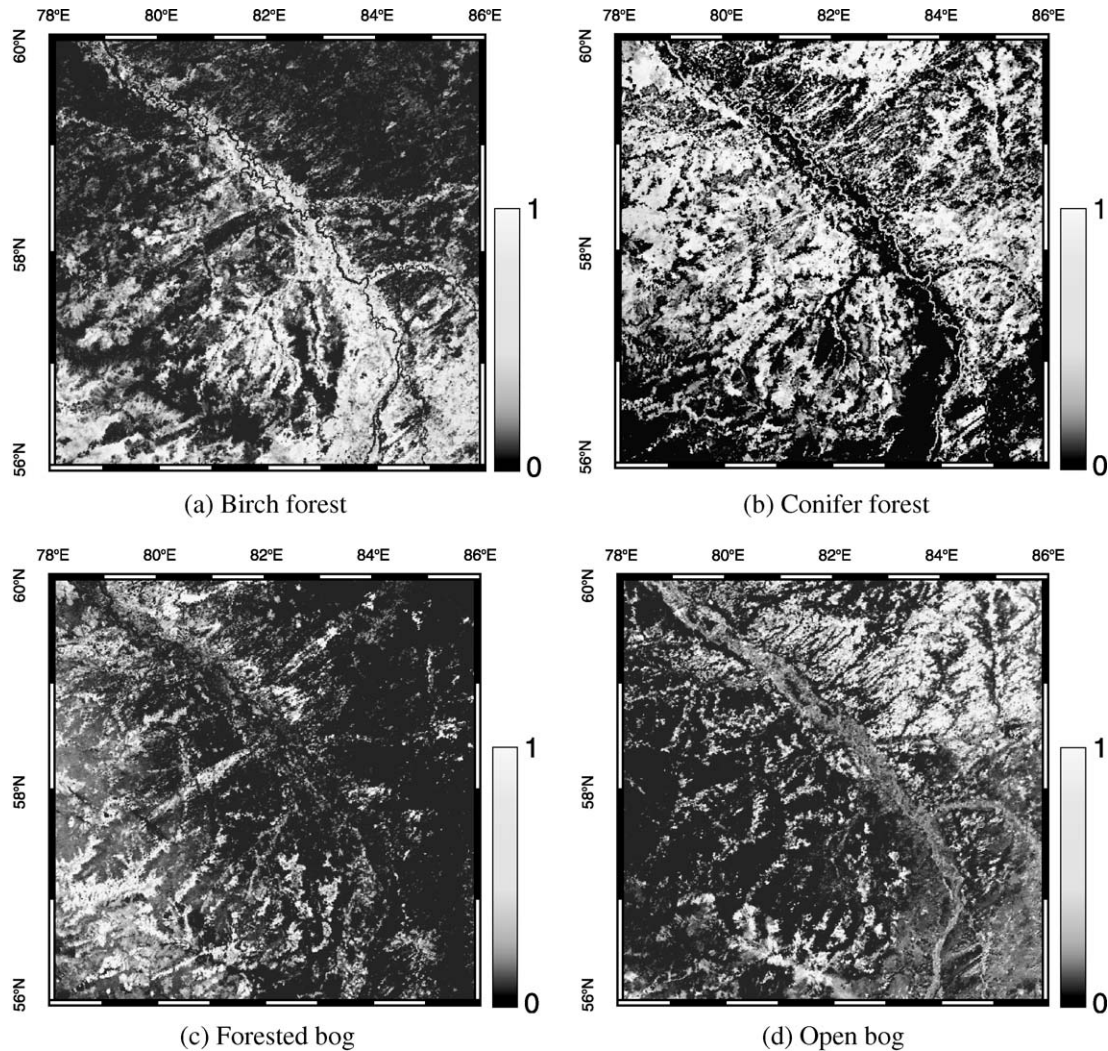
Fig. 5. Results of spectral mixture analysis of wetland ecosystems near Plotnikovo. Bright values indicate areas of high fractional abundance of that endmember.
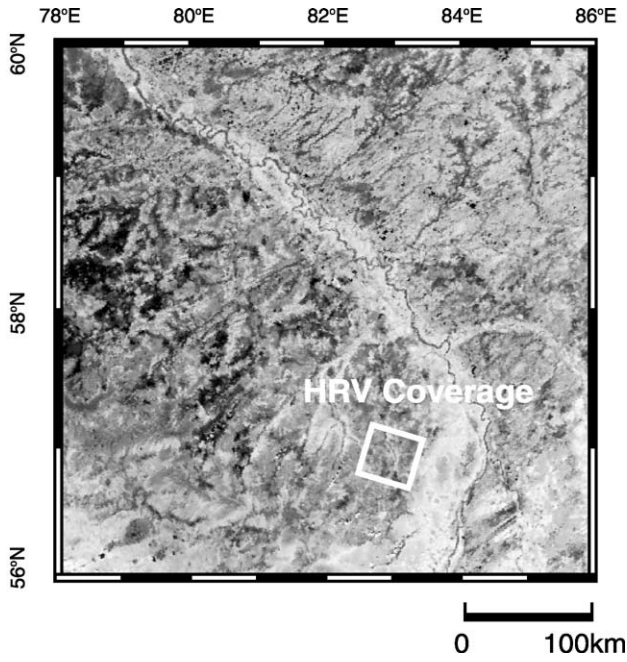
Fig. 6. NOAA AVHRR image over West Siberian wetland. The square shows the area covered by SPOT HRV.

The total methane flux F_{total} and the mean methane flux F_{mean} over AVHRR coverage are calculated respectively as follows from the sum

$$F_{total} = \sum_{i=1}^{n} A_i f_i \qquad (5-a)$$

$$F_{mean} = F_{total} \Big/ \sum_{i=1}^{n} A_i \qquad (5-b)$$

where n is a number of categories, A_i is a total area of each category and f_i is a methane emission rate of each category. Results of these calculations are shown in Table 3 for the studied area of AVHRR about 400×400 (km^2). The total methane flux over the AVHRR coverage was calculated to be 9.49 (10^9 g CH$_4$/day) and the mean methane flux over AVHRR coverage was calculated as 59.3 (mg CH$_4$/m^2/day).

4.5. Accuracy assessment

4.5.1. Evaluation of classification accuracy

The performance of the scaling model was evaluated in terms of the root mean squared (RMS) error. For the four

Table 1
Estimated areas of four ecosystems based on spectral mixture analysis between AVHRR and HRV

Category	Birch forest	Conifer forest	Forested bog	Open bog	Total
Areal ratio (%)	23.6	35.0	17.6	23.8	100.0
Area (10^3 km^2)	37.8	56.0	28.2	38.0	160.0

Table 2
Mean methane fluxes measured on the ground in July of 1993 and 1994

Site	Number of measurement points	Mean flux (mg CH$_4$/m^2/day)	S.D.
Forested bog	23	21.1	43.8
Open bog	56	233.1	326.1

given classes (birch forest, conifer forest, forested bog and open bog), the RMS error with respect to that class is as follows

$$E_k = \sqrt{\frac{1}{N_p} \sum_{n=1}^{N_p} (B_{k,n} - B_{k,n}^*)^2} \qquad (6-a)$$

$$E_t = \frac{1}{N_p} \sum_{n=1}^{N_p} \sqrt{\frac{1}{N_k} \sum_{k=1}^{N_k} (B_{k,n} - B_{k,n}^*)^2} \qquad (6-b)$$

where $B_{k,n}$ is the original fraction value of category k of pixel n, $B_{k,n}^*$ the estimated fraction value, N_p the number of pixels and N_k the number of categories.

The results of the classification accuracy are presented in Table 4. Overall, the accuracies were tolerably high and consistent across the individual classes. Individual class accuracies reveal that birch forest is the most accurately identified ecosystem category followed by open bog, forested bog and conifer forest (Fig. 7). The validation described above is obviously incomplete in that it relies entirely on the classification result with SPOT HRV data and the assumption that the all the pixels of HRV are pure pixels. The inability of the validation method to quantify the uncertainty of other neglected categories is a significant issue and must be resolved in future studies. In spite of the acknowledged inability of the validation method to constrain the number of categories, this may be a real limitation imposed by the satellite data. Another error source of the mixture analysis is the use of AVHRR channel 3 in the daytime. Specifically, it contains both emitted and reflected energy, and hence, can add uncertainty in the derived land cover fractional maps (i.e., two land covers could produce the same AVHRR-3 value, where one is primarily contributing reflected energy and the other emitted energy).

Table 3
Methane emission from 400×400 (km^2) of study area

Category	Area (10^3 km^2)	Emission rate (mg CH$_4$/m^2/day)	Total flux (10^9g CH$_4$/m^2/day)
Birch forest	37.8	0.0	0.0
Conifer forest	56.0	0	0.0
Forested bog	28.2	21.1	0.60
Open bog	38.0	233.9	8.89
Total	160.0	–	9.49

Table 4
Evaluation of classification accuracy by simple percent agreement value

Category	Birch forest	Conifer forest	Forested bog	Open bog	Total
Error (%)	19.2	19.4	19.3	17.9	19.0
Correlation coefficient	0.889	0.723	0.732	0.841	–

4.5.2. Evaluation of the methane emission

Here we discuss the methane emission variability. Table 2 shows that the temporal dynamics were chaotic: no correlation between particular chambers were observed. The methane emission of forested bog was statistically calculated as 21.1 ± 43.8 (mg CH_4/m^2/day) and that of open bog as 233.9 ± 326.1 (mg CH_4/m^2/day). Net flux of CH_4 from boreal and sub-arctic peat lands to the atmosphere is difficult to estimate, and thus, there are uncertainties in determining how many different types of measurements are needed to characterize the source (Morrissey & Livingston, 1992). As with temperate and sub-tropical wetlands, methane emission fluxes from northern wetlands are extremely variable. CH_4 estimates are affected strongly by pH, temperature and depth of water table (Macdonald et al., 1998); however, the correlation between methane emission and such environmental factors was found to be very low (determination coefficient less than 0.11) (Panikov et al., 1997). Thus, the only valuable predictor among available soil-ecological indicators can be vegetation covers.

Tohjima et al. (1994) estimated the methane fluxes over HRV coverage from the measurements of vertical profiles. Table 5 shows accumulated methane, accumulation period

Table 5
Regional methane fluxes estimated from the methane vertical profiles (Tohjima et al., 1994)

Date	Accumulated methane (mg/m^2)	Accumulation period (hour)	Methane flux (mg CH$_4$/m^2/day)
August 3, 1994	55	15	88
August 5, 1994	20	14	34
August 6, 1994	79	15	126
Average	–	–	83

and estimated regional methane fluxes for 3 measurement days. They have large variations from 34 to 126 (mg CH_4/m^2/day). This large variation means spatial and temporal variability of methane concentration. The average methane flux for 3 days of observations was 83 (mg CH_4/m^2/day), which is about 1.4 times larger than our estimate 59.3 (mg CH_4/m^2/day) calculated from the combination of remote sensing analysis and ground measurements. This discrepancy might be partly because of neglecting the contributions from water. However, if we note that both estimates are based on measurement results with large variations, we could conclude that our result is well within the range of probabilistic variability.

5. Summary

This study demonstrated that scaling techniques would provide a tool to extrapolate the local information from high spatial resolution data to larger scale by using low spatial resolution data. Firstly, spectral mixture analysis was conducted between NOAA AVHRR and SPOT HRV and four

(a) Birch forest

(b) Conifer forest

(c) Forested bog

(d) Open bog
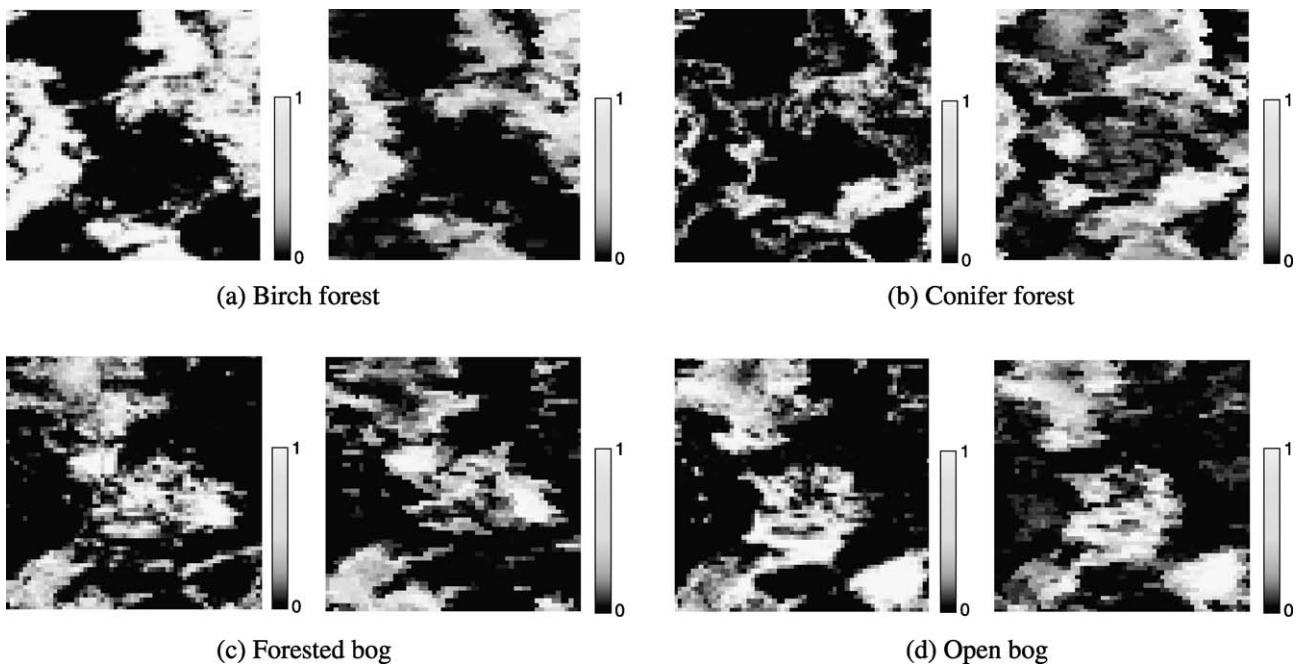
Fig. 7. Classification accuracy of mixture fractions of each category. Bright values indicate areas of high fractional abundance of that endmember (left, aggregated classification image from HRV; right, estimated fraction image from AVHRR).

wetland ecosystems (birch forest, conifer forest, forested bog and open bog) distribution was estimated with sub-pixel level. Then, the total methane flux over AVHRR coverage was estimated with the combination of remote sensing classification and the ground methane measurement results. Finally, the mean methane flux over AVHRR area was calculated to be 59.3 (mg CH_4/m^2/day), which is within the range of probabilistic variability as compared with airborne measurement results.

As most of the global issues including deforestation or desertification originate from local events, monitoring earth surface changes requires that the observation of land cover should examine the terrain from local to global scale. Linking local with global is one of the key aspects in tackling global environmental issues and the method proposed in this study contributes toward realizing the bridge between the local and the global in remote sensing.

Acknowledgements

References

Asner, G. P., Wessman, C. A., & Priette, J. L. (1997). Unmixing the directional reflectances of AVHRR sub-pixel land covers. *IEEE Trans. Geosci. Remote Sens., 35*, 868–878.

Bartlett, K. B., & Harris, R. C. (1993). Review and assessment of methane emissions from wetlands. *Chemosphere, 26*, 261–320.

Bateson, C. A., Asner, G. P., & Wessman, C. A. (2000). Endmember bundles: a new approach to incorporating endmember variability into spectral mixture analysis. *IEEE Trans. Geosci. Remote Sens., 38*, 1083–1094.

Crill, P. M., Bartlett, K. B., Harriss, R. C., Gorham, E., Verry, E. S., Sebacher, D. I., Mazdar, L., & Sanner, W. (1988). Methane flux from Minnesota peatlands. *Glob. Biogeochem. Cycles, 2*, 317–384.

Elman, H. C., & Golub, G. H. (1994). Inexact and preconditioned Uzawa algorithms for saddle point problems. *SIAM J. Numer. Anal., 31*, 1645–1661.

Floudas, C. A., & Visweswaran V. (Eds.) (1995). *Quadratic optimization: handbook of global optimization* (pp. 217–269). Kluwer Academic Publishers.

Goodrum, G., Kidwell, K. B., Winston, W. (Eds.) (1999, May). NOAA KLM User's guide.

Houghton, J. T., Meira Filho, L. G., Callander, B. A., Harris, N., Kattenberg, A., & Maskell, K. (Eds.) (1998). *Climate Change 1995: the Science of Climate Change*. New York: Cambridge University Press.

Macdonald, J. A., Fowler, D., Hargreaves, K. J., Skiba, U., Leith, I. D., & Murray, M. B. (1998). Methane emission rates from a northern wetland; response to temperature, water table and transport. *Atmos. Environ., 32*, 3219–3227.

Morrissey, L. A., & Livingston, G. P. (1992). Methane emissions from Alaska arctic tundra: an assessment of local spatial variability. *J. Geophys. Res., 97*, 16661–16670.

Oleson, K. W., Sarlin, S., Garrison, J., Smith, S., Privette, J. L., & Emery, W. J. (1995). Unmixing multiple land-cover type reflectances from coarse spatial resolution satellite data. *Remote Sens. Environ., 54*, 98–112.

Panikov, N. S. (1994). CH_4 and CO_2 emission from northern wetlands of Russia. *Proc. of the Int. Symposium on Global Cycles of Atmospheric Greenhouse Gases* (pp. 100–112).

Panikov, N. S., Glagolev, M. V., Kravchenko, I. K., Mastepanov, M. A., Kosych, N. P., Mironycheva-Tokareva, N. P., Naumov, A. V., Inoue, G., & Maxutov, S. (1997). Variability of methane emission from West Siberian wetlands as related to vegetation type. *Ecol. Chem., 6*, 59–67.

Price, J. C. (1999). Combining multi-spectral data of differing spatial resolution. *IEEE Trans. Geosci. Remote Sens., 37*, 1199–1203.

Shimabukuro, Y. E., & Smith, J. A. (1991). The least-squares mixing models to generate fraction images derived from remote sensing multi-spectral data. *IEEE Trans. Geosci. Remote Sens., 29*, 16–20.

Shimoda, H., Fukue, K., Cho, K., Matsuoka, R., Hashimoto, T., Nemoto, T., Tokunaga, M., Tanba, S., & Takagi, M. (1998). Development of a software package for ADEOS and NOAA data analysis. *Proceedings of the IGARSS 1998, vol. 2* (Int. 03).

Singh, S. N., Kulshreshtha, K., & Agnihotri, S. (1991). Seasonal dynamics of methane emission from wetlands. *Glob. Chang. Sci., 29*, 16–20.

Tamura, M., & Yasuoka, Y. (1998). Extraction of wetland areas in the West Siberian Lowland using NOAA/AVHRR imagery. *Proc. of the Seventh Symposium on the Joint Siberian Permaforest Studies Between Japan and Russia* (pp. 40–46).

Tohjima, Y., Maksyutov, S., Machida, T., & Inoue, G. (1994). Airborne measurement of atmospheric CH_4 over the West Siberian Lowland during the 1994 Siberian Terrestrial Ecosystem–Atmosphere–Cryosphere Experiment (STEACE). *Proc. of the Third Symposium on the Joint Siberian Permaforest Studies Between Japan and Russia* (pp. 50–57).